The heterogeneity of olfactory ensheathing cell interactions is regulated by lamellipodial waves

Journal:	*GLIA*
Manuscript ID:	Draft
Wiley - Manuscript type:	Original Research Article
Date Submitted by the Author:	
Complete List of Authors:	Windus, Louisa; Griffith University, National Centre for Adult Stem Cell Research; The University of Queensland, School of Biomedical Sciences Lineburg, Katie; Griffith University, National Centre for Adult Stem Cell Research Scott, Susan; Griffith University, National Centre for Adult Stem Cell Research Claxton, Christina; The University of Queensland, School of Biomedical Sciences Mackay-Sim, Alan; Griffith University, National Centre for Adult Stem Cell Research Key, Brian; The University of Queensland, School of Biomedical Sciences St John, James; Griffith University, National Centre for Adult Stem Cell Research
Key Words:	olfactory bulb, axon, lamina propria, adhesion, regeneration

Note: The following files were submitted by the author for peer review, but cannot be converted to PDF. You must view these files (e.g. movies) online.

Movie 1.wmv
Movie 2.wmv
Movie 3.wmv
Movie 4.wmv

The heterogeneity of olfactory ensheathing cell interactions is regulated by lamellipodial waves.

Louisa C.E. Windus[1,2], Katie E. Lineburg[1], Susan E. Scott[1], Christina Claxton[2], Alan Mackay-Sim[1], Brian Key[2], James A. St John[1]*

1. National Centre for Adult Stem Cell Research, Eskitis Institute for Cell and Molecular Therapies, Griffith University, Australia.
2. School of Biomedical Sciences, The University of Queensland, Brisbane, Queensland, Australia

Running title: OECs are a heterogeneous population

Number of words: Abstract = 250; Introduction = 591, M&M = 1031, Results = 3285, Discussion = 1238, Acknowledgments = 49, Bibliography = 834, Legends = 1869.
Number of figures: 7, with 4 supplemental movies
Number of tables: 0

*Corresponding author:
Dr James St John
National Centre for Adult Stem Cell Research
Eskitis Institute for Cell and Molecular Therapies
Griffith University
Nathan 4111
Brisbane
Queensland
Australia

email: j.stjohn@griffith.edu.au
phone: +61 7 3735 3660, Facsimile: +61 7 3735 4255

Key words: olfactory bulb, axon, lamina propria, adhesion, regeneration

Abstract

The regenerative capacity of the olfactory system is attributed to the presence of olfactory ensheathing cells (OECs) as they are intimately associated with primary olfactory axons from the olfactory epithelium to the olfactory bulb. However, OECs are not a uniform population of cells. They express distinct markers and are thought to play different roles depending on their anatomical position. As OECs arise from a common progenitor and migrate to populate the primary olfactory nerve, the different subpopulations must intermingle and sort out with considerable cell-cell interactions occurring. However, little is understood about how OECs interact and how the different subpopulations of OECs are capable of detecting and responding to each other. We have microdissected anatomically distinct subpopulations of OECs from the olfactory bulb and from the peripheral nerve and performed cell behaviour assays. We reveal that the behaviour of OECs dramatically alters depending on their anatomical location and developmental age. In particular, centrally-derived OECs are a heterogeneous population of cells that respond to cell-cell contact with a mix of adhesive, repulsive and indifferent responses. In contrast, OECs derived from the peripheral olfactory nerve are a homogeneous population. We have further determined that lamellipodial waves along the shaft of centrally-derived OEC processes are imperative for initiating and mediating behaviour during cell-cell contact. Inhibition of lamellipodial waves via Mek-1 resulted in OECs losing the ability to differentiate between subpopulations. These results demonstrate that centrally-derived OECs are a heterogeneous population of cells and that cell-cell recognition and responses are regulated through lamellipodial waves.

INTRODUCTION

The primary olfactory system is one of few regions within the mature vertebrate nervous system to exhibit continual turnover of neurons and a capacity for axon growth throughout life. Regenerating primary olfactory sensory neurons extend axons through a transitional zone between peripheral and central nervous systems in order to reach their targets in the olfactory bulb. This regenerative capacity has been attributed to the presence of a specialised population of macroglia called olfactory ensheathing cells (OECs), which populate the peripheral olfactory nerve and outermost layers of the olfactory bulb in the central nervous system (Chuah and Au 1991; Doucette 1984; Farbman and Squinto 1985). OECs are thus believed to play a role in the establishment and maintenance of the olfactory nerve and in the sorting of axons within the nerve fibre layer of the olfactory bulb (Doucette 1989; Farbman and Squinto 1985; Valverde et al. 1992).

OECs are often classified into two broad categories: peripheral OECs and central OECs. Peripheral OECs ensheathe the fascicles of mixed primary olfactory axons that project from the olfactory epithelium to the olfactory bulb. Peripheral OECs are thought to be crucial for the growth, guidance and survival of olfactory axons as they extend towards the olfactory bulb (Doucette 1990). En route to the bulb these fascicles penetrate the cribriform plate and enter the outer layer of the olfactory bulb, the nerve fibre layer (NFL), which lies within the central nervous system. The primary olfactory axons then defasciculate from the mixed bundles of axons, sort out and refasciculate with axons that express the same odorant receptor (Mombaerts et al. 1996). In this way, axons that arise from neurons expressing the same odorant

receptor fasciculate together and finally project to their target glomeruli. The central OECs populate the NFL and are believed to contribute to the complex sorting of axons within this layer.

The origin of the primary olfactory system lies in the olfactory placode that gives rise to the primary olfactory neurons and OECs (Chuah and Au 1991). Hence the OECs migrate, along with the axons, from the olfactory epithelium to populate the peripheral nerve and the NFL of the olfactory bulb. While the peripheral and central OECs share many characteristics it is known that the expression of various markers differs between the OECs that reside in the peripheral nerve and those within the NFL (Vincent et al. 2005a). These differences in expression are likely to be conferred upon the OECs by the anatomical position they are targeting but may also be predetermined by the differential expression of transcription factors at their point of origin. Regardless of whether the expression of the markers is regulated by anatomical position or transcription factors, the migrating subpopulations of OECs need to undergo considerable cell-cell interactions during development of the olfactory system.

We have previously reported that lamellipodial waves on peripheral OECs regulate cell-cell interactions and overwhelmingly lead to adhesion between peripheral OECs; and that the waves also contribute to OEC migration. We have now examined the behaviour of cell-cell interactions of peripheral OECs and four different anatomical subpopulations of central OECs throughout development. We have determined for the first time that peripheral and central OEC subpopulations display very different behaviours during cell-cell contact and that the cell recognition and resultant

behaviour is regulated via lamellipodial waves. Loss of wave activity perturbs the ability of OECs to recognise and interact with each other. These results demonstrate that OECs are a heterogeneous population of cells and that the resultant behaviours of OEC cell-cell interactions are consistent with their proposed roles in vivo.

MATERIALS AND METHODS

Generation of OMP-ZsGreen transgenic mice

Transgenic mice expressing ZsGreen in olfactory sensory neurons were generated. In these mice, the full length (5.5kb) olfactory marker protein (OMP) promoter (Danciger et al. 1989) drove the expression of ZsGreen fluorescent protein, from pZsGreen- Express Vector (Clontech, Palo Alto, CA). Olfactory marker protein (OMP) is selectively expressed at high levels in mature olfactory sensory neurons (Margolis 1972). The transgene was liberated from the vector using EcoR1 restriction sites and injected into fertilised mouse oocytes at the Transgenic Animal Service of Queensland (University of Queensland, Brisbane). Successful integration of the transgene was confirmed by expression of ZsGreen fluorescence in the olfactory system of living neonatal animals. In these animals the vast majority of primary olfactory neurons express ZsGreen. The OMP-ZsGreen mice were then crossed with S100ß-DsRed transgenic mice (Windus et al. 2007) (Fig. 3). All procedures were carried out with the approval of, and in accordance with, the Griffith University Animal Ethics Committee, the University of Queensland Animal Ethics Experimentation Committee and the Australian Commonwealth Office of the Gene Technology Regulator.

Immunohistochemistry

Adult S100ß-DsRed mice (Windus et al. 2007) were asphyxiated by CO_2 and heads were fixed in 4% paraformaldehyde and sectioned (30 μm) on a cryostat microtome. Immunohistochemistry was performed as previously described (Windus et al. 2007) and incubated with either polyclonal rabbit anti-p75NTR (1:500; Chemicon, Temecula, CA) or polyclonal rabbit anti-NPY (1:400; DakoCytomakon, Denmark) or

polyclonal rabbit anti-human S100ß (1:1000; DakoCytomation, Glostrup, Denmark), followed by goat anti-rabbit secondary antibodies conjugated to biotin (1:200; Vector Labs, Burlingame, CA) and then with Streptavidin-conjugated Alexa Fluor^{488} (1:400; Molecular Probes, Carlsbad, CA).

Isolation of OECs from the lamina propria and olfactory bulb

Embryonic day 17 (E17) and postnatal day 2.5 (P2.5) S100ß-DsRed mice were killed by decapitation; adult mice were killed by CO_2 asphyxiation. Peripheral OECs were isolated from the lamina propria underlying the neuroepithelium of the posterior half of the nasal septum. Fine forceps were used to tease away large olfactory nerve fascicles from the lamina propria (LP). Central OECs were prepared from the nerve fibre layer (NFL) of the olfactory bulbs. To obtain central OECs from the entire NFL, the olfactory bulb was removed from the cranial cavity and the NFL from the entire bulb was dissected. To obtain rostral, dorsal, caudal and ventral derived OECs, the NFL was directly taken from the corresponding anatomical regions (Fig. 3a). The LP or NFL tissue were incubated in plastic 24-well plates coated with Matrigel basement membrane matrix (10 mg/ml; BD Biosciences, San Jose, CA) and maintained in Dulbecco's Modified Eagle Medium containing 10% fetal bovine serum (E17 and P2 tissue) or 20% fetal bovine serum (adult tissue), G5 supplement (Gibco), gentamicin (Gibco, 50 mg/ml) and L-glutamine (200 μM) at 37°C with 5% CO_2 for 3-5 days (E17 and P2) or 2 weeks (adult). Contaminating macrophages were removed by incubation with TrypLE Express (Gibco) for 2 min. OECs were incubated with TrypLE Express for a further 4-5 min and then transferred to glass-bottomed 24-well plates coated with Matrigel and maintained in the same medium. All time-lapse images were collected after 24-72 hr of the first plating.

Growth factor and inhibitor assays of central OECs

OECs were incubated with each of the following: recombinant rat Glial cell line-derived neurotrophic factor (GDNF, Bio-Scientific, NSW, Australia), Nerve Growth Factor (NGF, Invitrogen Corporation, Melbourne, Australia) at final concentrations of 10 ng/ ml and 20 ng/ml, JNK inhibitor II SP600125 (50 nM, Sigma-Aldrich), Src family kinase inhibitor PP2 (5 µM; Calbiochem, Merck, Darmstadt, Germany), the inactive analogue PP3 (5 µM; Calbiochem), Rac 1 inhibitor (NSC23766, 5 µM, 10 µM Calbiochem), Mek 1 inhibitor (Ethanolate U0126; 5 µM, 10 µM, 20 µM Sigma-Aldrich).

Axon outgrowth assay

Monolayers of either central or peripheral derived OECs were plated on glass-bottomed 24-well plates coated with Matrigel and maintained for 8 hr in the same medium as described above. Explants of olfactory neuroepithelium from E12-E14 OMP-ZsGreen mice were then plated directly onto the monolayer. The medium was changed and explants were then maintatined in Neurobasal medium (GIBCO) supplemented with B27 (20 µl/ml), L-glutamine (4 µl/ml), 5 µl/ml of gentamycin at 1mg/ml, HEPES (10 µl/ml at 10 mM) and N-methyl Cellulose 100 µl/ml. Axon outgrowth occurred within 24 hr.

Time-lapse and fixed tissue imaging

Time-lapse images were routinely collected at intervals of 15-30 s over periods of 40 - 60 min using an AxioCam MRm digital camera and a Uniblitz VCM01 shutter on an inverted Zeiss Axioobserver Z1 microscope fitted with epifluorescence and

differential interference contrast optics. Images were collected with a Zeiss LD PlanNeo-FLUAR 25/0.8 water iris and a LD PlanNeo-FLUAR 20/0.75 air iris. During imaging culture plates were maintained at 37 °C in an incubator chamber with 5% CO_2. Images were compiled using Axiovision Rel 4.6.3 (Zeiss, Germany) and colour-balanced in Adobe Photoshop v 10.0 without further digital manipulation. Images of fixed tissue were collected on a Zeiss AxioImager Z1 with an Axiocam MRm digital camera using Axiovision software (Zeiss, Germany) and Zeiss EC Plan-NeoFLUAR 20/0.75 air iris and an EC Plan-NeoFLUAR 5/0.15 air iris or on an Olympus IX81 scanning confocal microscope, using Olympus Fluoview Ver 1.7b software (Olympus, Tokyo).

Quantification of wave processes and migration rates

Time-lapse image sequences of primary OEC cultures were collected and analysed with Axiovision Rel 4.6.3 (Zeiss, Germany). The distance measurement tool was used to trace the rate and direction of waves on cell processes. The average journey rate was defined as the total distance individual waves travelled over the total recording time. The number of waves that occurred on cell processes was summed over the 1 hr recording period. Waves were measured only when they were clearly distinguishable from the leading edge of both the process upon which it travelled and adjacent cells. The migration rate of any given cell was calculated by tracing the total distance travelled by the cell body over the total recording period; a measure obtained using the Axiovision distance measurement tool.

Statistical analyses

Statistical significance for the migration rate was tested using a Kruskal-Wallis test and Dunn's Multiple Comparison test for post-hoc analysis. Statistical significance for all other measurements was tested using either a Chi-square test or a Fishers exact test for two variables.

RESULTS

OECs are a heterogeneous population of cells.

In vivo OECs display distinct roles in the olfactory neuraxis; in the peripheral nervous system (PNS) OECs ensheathe and promote the growth of olfactory neuron axons in tightly fasciculated bundles as they exit the olfactory epithelium and extend towards the olfactory bulb (Fig. 1A); in the CNS OECs reach the outer nerve fibre layer (oNFL; Fig. 1B) and are intermingled with the axons as the axons undergo defasciculation and sorting out (Fig. 1A). In the inner NFL (iNFL; Fig. 1B) the OECs assist in the refasciculation of axons expressing the same odorant receptors (Fig. 1A).

Consistent with previous reports (Astic et al. 1998; Barnett et al. 1993; Valverde et al. 1992) we found that central and peripheral populations of OECs express different antigenic markers. Using coronal sections from adult S100ß-DsRed transgenic mice (Windus et al. 2007) we found that S100ß-DsRed is expressed by peripheral OECs in the olfactory nerve (ON; 1D, 1E) and by central OECs in both the oNFL and iNFL (Fig. 1B). Endogenous S100ß immunostaining (green fluorescence, Fig. 1C) was absent from the DsRed-positive iNFL (Fig. 1C). Since the distribution of endogenous S100ß varies across the depth of the NFL in different species (Au et al. 2002; Bailey et al. 1999; Gong et al. 1994) it was fortuitous that the human S100ß regulatory sequences used to drive expression of DsRed produced ubiquitous expression in OECs of the NFL. OECs in the iNFL were neuropeptide Y (NPY) positive (Fig. 1D) but lacked the low-affinity neurotrophin receptor p75 ^{NTR} (Fig. 1E). Anti-p75 ^{NTR} immunostaining was present on peripheral OECs throughout the olfactory nerve (Fig. 1E-F).

While it is clear that peripheral and central OECs have different roles and antigenic profiles in vivo (Huang et al. 2008; Schwarting et al. 2000; St John and Key 1999; St John and Key 2001; Storan et al. 2004; Vincent et al. 2005a), there is no experimental data to support a clear antigenic or functional distinction between theses two spatially different sources of OECs in vitro (Au and Roskams 2003; Jani and Raisman 2004; Kumar et al. 2005). In fact peripheral and central OECs have been shown to have remarkable similarities in vitro including similar phenotypes and molecular markers (see review by Vincent et al. 2005b). However we know little of how at the cellular level OECs interact with themselves or other cell types in vitro. Using high resolution timelapse microscopy we endeavoured to investigate whether there were differences in how central or peripheral derived OECs interacted with themselves or olfactory axons in vitro.

In order to selectively identify and visualise peripheral OECs derived from the lamina propria and central OECs derived from the olfactory bulb for time-lapse studies, we cultured cells from S100ß-DsRed transgenic mice (Windus et al. 2007) and maintained the cells in culture for one passage only. In culture there were striking differences between the two populations of OECs. Central OECs were spatially dispersed (Fig. 1G) with a small proportion of cells in direct contact with each other. In comparison peripheral OECs were highly adhered with the majority of cells in close contact with each other (Fig. 1I). We next grew primary olfactory neurons cultured from the neuroepithelium of the OMP-ZsGreen transgenic line. When grown on a monolayer of central OECs, axons (Fig. 1H) were consistently spatially dispersed in comparison to axons grown on peripheral OECs (Fig. 1J). Axons grown on

peripheral OECs displayed a highly fasciculated and adherent phenotype (Fig. 1J). It was clear that olfactory axons migrated directly along the processes and cell body of OECs using them as a preordained migratory pathways (Fig. 1H, J arrows). Therefore the migratory behaviour of axons was determined primarily by the spatial orientation of the OECs. We therefore wanted to further investigate what mechanisms mediate these fundamental differences in OEC cellular behaviour.

Peripheral and central OECs respond differently to cell-cell contact

The more dispersed nature of the central OECs in vitro suggested that differences in adhesion/repulsion between cells could be occurring. We therefore tested whether subpopulations of OECs display differential cellular responses during cell-cell contact using in vitro assays that we have previously established (Windus et al. 2007). In these assays, primary cultures of OECs were replated at densities that allowed for high resolution time-lapse microscopy of cells as they are undergoing initial cell-cell contact and interactions.

We first examined the behaviour of peripheral OECs derived from E17, P2 or adult tissue. We consistently found that when two peripheral OECs initiated cell-cell contact, the interaction overwhelmingly led to adhesion (data not shown, but interaction is similar to that shown for central OECs in Fig. 2A). In the context of these time-lapse analyses, adhesion was defined as both processes remaining in contact with each other for at least one hour, which was the limit of our imaging sequences. This adhesive behaviour was consistent regardless of the age of the donor tissue (86-90% of interactions, Fig. 2D).

We next investigated OECs derived from the entire NFL of the olfactory bulb. To obtain these cells, the NFL from all regions of the olfactory bulb was cultured together including cells from the rostral, ventral, dorsal and caudal regions (see Fig. 3A). The behaviour of central OECs was remarkably different from peripheral OECs. When two central OECs initiated cell-cell contact, the interactions resulted in a mix of behaviour including adhesion (Fig. 2A), repulsion (Fig. 2B) or would continue growing over each other without exhibiting any adhesion or repulsion (cross-over Fig. 2C). During adhesive interactions, the leading edge of one OEC (Fig. 2A arrow) would contact the shaft of another OEC (Fig. 2A asterisk). The two processes would actively interact with each other (Fig. 2A 04.17 – 9.27 arrows, arrowheads) which resulted in the fusion of two OEC processes (Fig. 2A, 45.16, asterisk; Supplementary movie 1). Typically during repulsive interactions, the leading edge of an OEC process (Fig. 2B arrow) would approach the shaft of another OEC (Fig. 2B asterisk), make initial contact (Fig. 2B; 16.42 arrow) but then actively withdraw from the shaft (Fig. 2B; 33.42 arrow) and make no further contact (Supplementary movie 2). Typically during a cross-over interaction, two OEC processes would interact with each other (Fig. 2C arrowhead) but the processes would continue to migrate along different paths without adhering or repelling from each other (Fig. 2C; 06.40-40.00; Supplementary movie 3).

When derived from embryonic tissue, cell-cell contact of central OECs resulted in an equal mix of adhesion (32%), repulsion (38%) or continued growth to cross-over each other without exhibiting any adhesion or repulsion (cross-over, 30%; Fig. 2E).

Interestingly, when derived from postnatal or adult mice, central OECs had increased adhesion responses (58% P2, 54% adult; Fig. 2E) but maintained their repulsion responses. Thus the increase in adhesion responses was at the expense of cross over responses. However, at no age were the responses similar to the peripheral OECs, which always overwhelmingly resulted in adhesion (Fig. 2D).

These results suggest that:

1. peripheral OECs derived from tissue of all ages consist of a *homogeneous population* of cells that primarily adhere to one another during cell-cell contact;
2. central OECs consist of a heterogeneous population of cells that exhibit a mix of *three distinct behaviours:* a) adhesion, b) repulsion or c) cross-over.

Subpopulations of central OECs respond differently to cell-cell contact

The development of the central region of the olfactory system is not uniform. At E11 the very rostral region of the presumptive nerve fibre layer (NFL) of the murine olfactory bulb is the first to develop. Nascent glomeruli become evident at E17 (Fig. 3A) and they develop across a gradient from rostral to caudal with this pattern continuing into postnatal and adult (Fig. 3D, G). Moreover, the transition zone between the peripheral and central olfactory system lies in the rostral and ventral regions of the olfactory bulb (Fig. 3A, arrowheads) where axons primarily defasciculate and sort out, especially during embryonic and early postnatal development. In contrast, the NFL of the dorsal and caudal regions is much thinner and glomeruli develop later in these regions (Fig. 3F, I). Based on these anatomical development differences, we hypothesised that the OECs cultured from distinct topographical locations of the olfactory bulb may also exhibit behaviourally different

responses to cell-cell contact. Further, we rationalised that these differences would vary across different developmental stages. To investigate this, central OECs were cultured from rostral, dorsal, ventral and caudal regions of the NFL derived from E17, P2 or adult animals.

We first examined OECs from the rostral NFL and found that when derived from E17 tissue, cell-cell contact predominantly resulted in repulsion (60% Fig. 3J). However when cultured from P2 tissue, cell-cell contact between rostral OECs resulted in more of a mix of adhesion (45%), repulsion (35%) and cross-over events (20%) (Fig. 3D). Similarly, when derived from adult tissue an even mix of adhesion, repulsion and cross-over occurred. We can infer from these results that rostral OECs consistently display a mix of the three distinct behaviours throughout development.

We next examined OECs from the dorsal NFL. When derived from embryonic animals, these OECs displayed an equal mix of adhesion (35%), repulsion (35%) and cross-over (30%) (Fig. 3K). Interestingly, when taken from P2 and adult tissue, dorsal OECs displayed an increase in adhesive events (57% at P2 and 56% at adult) while cross-over events significantly decreased (8% at P2 and 0% at adult). However, repulsive events remained constant across all developmental stages.

Similar results were found for OECs cultured from the ventral region of the NFL. Embryonic ventral OECs displayed a mix of adhesion (25%), repulsion (25%) and cross-over (50%) (Fig. 3L). However for postnatal and adult OECs the rates of adhesive events increased (60% at P2 and 45% at adult), while cross-over events significantly decreased (Fig. 3L).

Similar to dorsal and ventral OECs, caudal OECs derived from embryonic tissue exhibited an equal mix of responses to cell-cell contact: adhesion (33%), repulsion (33%) or cross-over (33%) (Fig. 3M). However, when taken from postnatal and adult tissue the predominant response was adhesion (71-83% respectively). Thus the caudal OECs derived from postnatal and adult tissue exhibited a more homogeneous response, and were similar to OECs derived from peripheral olfactory nerve.

These results clearly demonstrate that OECs located within different regions of the NFL display distinct behavioural differences. Of particular note, OECs from the rostral NFL exhibit an equal mix of behaviours into adulthood whereas OECs from the caudal NFL display predominantly adhesion events.

Central OECs display dynamic lamellipodial waves

We have previously shown that novel lamellipodial protrusions, termed lamellipodial waves, exist on the shafts of peripherally derived OECs and are crucial for mediating cell-cell contact and migration (Windus et al. 2007). We therefore wanted to investigate whether centrally derived OECs exhibited these waves. Consistent with our previous work, we found that the dynamic lamellipodia were present along the shaft and/or cell body of central OECs (Fig. 4A) and that these lamellipodial waves were distinct from the leading edge (Fig. 4A; asterisk). The waves were not constantly present, but rather periodically appeared along the OEC shaft (Fig. 4A; 00:46:22; dashed line) and travelled in both retrograde (Fig. 4A; 00.02.21 – 00.24.41 arrowheads) and anterograde (Fig. 4A; 00.46.22-00.53.26, unfilled arrowhead) directions. Moreover, these waves were found to rapidly and dynamically move along

the shaft in opposing directions (Fig. 4A; 00.53.26; anterograde wave –unfilled arrowhead; retrograde wave – dashed line) and would merge together on the OEC process (Fig. 4A; 01.04.26, arrow; Supplementary movie 4).

Lamellipodial waves initiate cell-cell contact

We have previously observed that when peripheral OECs interacted with each other, lamellipodial waves mediated most of the initial direct cell-cell contacts, and that without lamellipodial waves cell-cell adhesion did not occur (Windus et al. 2007). We have now examined the effect that the age of tissue has on the behaviour of lamellipodial waves and the resultant cell response.

For peripheral OECs derived from E17, P2 or adult tissue we found that the overwhelming majority of lamellipodial wave interactions resulted in cell-cell adhesion (Fig. 4B). Interestingly, when derived from E17 tissue all initial cell-cell contact events occurred only in the presence of waves. For example, when the leading edge of one OEC approached a neighbouring OEC it would very selectively contact a lamellipodial wave on the other cell; it would never contact the shaft directly if a wave was not present. However, in OECs derived from older animals, lamellipodial waves were not always involved in initial cell-cell contact although they were still involved in ~70% of interactions with the majority of these interactions resulting in stable adhesive contacts (Fig. 4B). During adhesive interactions, a lamellipodial wave was often seen at the point of interaction between the leading edge of one OEC and the shaft of another (Fig. 2A; 00.00, dashed line; 04.17; arrow). The lamellipodial wave would actively interact with and engulf the leading edge resulting in the fusion of two OEC processes (Fig. 2A 45.16, asterisk). It should be noted that repulsive

events did occur regardless of the age of the tissue however only around 10% of processes were found to display this behaviour (Fig. 2D). During repulsive interactions, the wave was seen to first expand towards the in-coming leading edge (Fig. 2B, 16.42; leading edge – arrow; wave – dashed line) before it rapidly reduced in size as the leading edge retracted (Fig. 2B, 33.42, arrow). These results suggest that lamellipodial waves are mechanisms for maintaining the intrinsic adhesive behaviour of peripheral OECs throughout development.

The behaviour of central OECs was remarkably different from peripheral OECs. While lamellipodial waves were similarly involved in 70-80% of all initial cell-cell interactions regardless of the age of donor tissue, the resultant cell response was varied. For E17 central OECs, there was an equal distribution of adhesive (38%), repulsive (26%) and cross-over events (36%) (Fig. 2E). Wave-based interactions from older animals resulted in increased adhesion (P2 68%; adult 61%; Fig. 4C), however a quarter to a third of interactions resulted in repulsion. Thus wave-based interactions on central OECs continued to result in a mix of cell responses. More importantly, lamellipodial waves were consistently involved in initiating cell-cell contact during all behaviours including adhesion, repulsion and even cross-over events (Fig. 4C). During cross-over events, a leading edge would briefly explore the lamellipodial wave before continuing directly over the process without adhering or repulsing. In some instances, after the leading edge had crossed over the process, lamellipodial waves would continue to survey the point of contact between the two processes (Fig. 2C, 00.00, arrowhead). It is worth noting that similar to peripheral E17 derived OECs, all central adhesive events occurred in the presence of lamellipodial waves (100% n=21/21).

In summary these results suggest that peripheral and central OECs have intrinsic differences in their cell behaviour following cell-cell contact and there is a clear bias for lamellipodial waves to initiate cell-cell contact between OECs. In embryonic animals lamellipodial waves were always involved in mediating adhesion of OECs. Next we wanted to investigate whether lamellipodial waves were crucial mechanisms in establishing cell-cell contact behaviour by modulating their behaviour independently of the leading edge.

GDNF regulates wave activity but does not change behaviour of central OECs

Glial cell line-derived neurotrophic factor (GDNF) has been shown to mediate migration of OECs by binding to GFRα-1 and Ret and subsequently activating JNK and SRC kinases (Cao et al. 2006). Previously we have reported that the generation of lamellipodial waves on peripheral OECs influences their migration rate and the activity of these waves can be modulated by GDNF (Windus et al. 2007). We have now examined the role of GDNF on centrally derived OEC migration and wave formation in the presence of exogenous GDNF.

Consistent with our previous results, the addition of GDNF to central OEC cultures increased the rate of OEC migration 4-fold (Fig. 5A). Inhibition of GDNF based signalling with selective inhibitors of either JNK (Bennett et al.; Hanke et al. 1996) or SRC (Whitesides and LaMantia 1996; Windus et al.) decreased OEC migration by 2-fold (Fig. 5A). These results confirmed that GDNF is an important regulator of central OEC migration. It was also clear that GDNF had an effect on lamellipodial wave activity. Following the application of 10-20 ng/ml of GDNF, the number and

size of waves exhibited by central OECs significantly increased. In the presence of GDNF, around 80% of central OECs subsequently displayed waves (Fig. 5B). The selective action of GDNF was evident since nerve growth factor (NGF), which is also expressed by OECs (Lipson et al., 2003), did not elicit the same response (Fig. 5B). GDNF also increased the surface area of lamellipodial waves (Fig. 5C-D).

Since GDNF signalling involves both JNK and SRC we next tested whether inhibition of these kinases affected the behaviour of lamellipodial waves on central OECs. When OECs were incubated with the JNK inhibitor SP600125 or with the SRC inhibitor PP2, the percentage of OECs displaying lamellipodial waves was significantly reduced (Fig. 5E) whereas incubation with the inactive analogue PP3 had no effect. When central OECs were incubated with both GDNF (20 ng/mL) together with either SP600125 or PP2, the frequency of lamellipodial waves was reduced to control levels (Fig. 5E). The rescue of the phenotype by GDNF indicates that these kinases are acting downstream of this growth factor in central OECs.

We have reported here that lamellipodial waves are important mechanisms that mediate cell-cell contact between central OECs. We next tested whether application of GDNF would affect the intrinsic behaviour of central OECs during cell-cell contact. We have shown that when taken from the rostral region of the olfactory bulb, OECs continually display an equal mix of responses including adhesion, repulsion and cross-over (Fig. 2A-C; Fig. 3J). With the addition of exogenous GDNF the resultant behaviour of interacting rostral OECs remained constant (Fig. 5F). Whether administered at 10ng/ml or 20 ng/ml concentrations, exogenous application of GDNF did not disrupt or affect the intrinsic cell behaviour of interacting rostral derived

OECs (Fig 5F). Hence increasing the activity of waves via GDNF does not alter the cell response.

Mek mediates lamellipodial wave formation and intrinsic cellular behaviour.

We have previously reported that the activity of lamellipodial waves is regulated independently of the leading edge via the Mek intracellular pathway (Doucette 1989). We next investigated whether lamellipodial waves on rostrally derived OECs were regulated by similar intracellular signalling molecules. Consistent with peripheral OECs, we found that inhibition of Rac1 by NSC23766 significantly reduced the activity of leading edge activity but did not significantly affect lamellipodial waves on OECs (Fig. 6A-B). In contrast, Mek1 inhibition by ethanolate U0126 had the reverse response with no significanteffect on leading edge activity, but instead significantly decreased lamellipodial wave activity (Fig. 6E-F). Rostral OEC migration was significantly decreased when the leading edge (Fig. 6C) or lamellipodial wave formation (Fig. 6G) was inhibited. These results suggest that both the leading edge and lamellipodiual waves are integral in maintaining normal migration rates.

We next investigated whether specifically inhibiting lamellipodial waves altered the responses to cell-cell contact. As previously stated, rostral OECs continue to display a heterogenous mix of behaviour during cell-cell contact (Fig. 2A-C; Fig. 3J) irrespective of the age of the donor tissue. When the leading edge activity was reduced by inhibition of Rac 1, the resultant behaviour of interacting rostral OECs remained constant with an equal mix of adhesion, repulsion and cross-over (Fig. 6D). In contrast, when lamellipodial wave activity was reduced by inhibition of Mek at both 5μM and 10μM concentrations there was a significant decrease in adhesive

events and an increase in cross-over behaviour (Fig. 6H). Thus, inhibition of lamellipodial waves resulted in over 80% of rostral OECs becoming non-responsive to each other during cell-cell contact (Fig. 6H). These results suggest that lamellipodial waves are crucial cellular components in maintaining intrinsic behaviours during cell-cell contact.

DISCUSSION

We reveal here for the first time that there are intrinsic fundamental differences in the cellular behaviour of central versus peripheral derived OECs in vitro. We have shown that central OECs are not a uniform population of cells, but instead they are a heterogeneous population that exhibit a mix of responses including adhesion, repulsion or cross-over during cell-cell interactions. In contrast peripheral OECs are a uniform population of cells that exhibit a homogenous adhesive response. We have also shown that dynamic lamellipodial protrusions along the shaft of OECs are integral in mediating cell-cell interactions. Lamellipodial wave activity is independent of the leading edge of the cell and is stimulated by GDNF and regulated via Mek 1. Moreover, inhibition of lamellipodial waves altered the intrinsic behaviours of interacting OECs. Without the presence of waves, OECs became non-responsive to each other during cell-cell contact.

The difference in the adhesive responses of OECs is consistent with the proposed roles in the various anatomical locations within the olfactory system. In mouse, axons of olfactory sensory neurons leave the olfactory epithelium in fascicles that coalesce to form the olfactory nerve, with each fascicle being encased by OECs (Treloar et al. 2002). In the periphery, therefore, OECs migrate out and surround the primary olfactory axons to form tightly bundled fascicles. The in vitro assays demonstrated that peripheral OECs undergo cell-cell adhesion and contact mediated migration consistent with their in vivo role. Later in development, the olfactory sensory axons and OECs reach and fuse with the telencephalon and then migrate into the presumptive nerve fibre layer (NFL) of the olfactory bulb (Schwarting et al. 2000; St

John and Key 1999). In the NFL, axons defasciculate from their intermixed bundles and sort-out depending on the type of odorant receptor they express, and OECs are thought to contribute to the defasciculation and sorting process. OECs are known to differentially express axon guidance or adhesion molecules. For example, semaphorin 3A is expressed in the ventral NFL but is absent from regions where axons that express neuropilin-1 enter the NFL (St John and Key 2001); the carbohydrate binding protein galectin-1 is widely expressed by OECs in the ventral/medial NFL, but is sparsely expressed in the dorsal/lateral NFL (Au et al. 2002); and ephrin-B2 is strongly expressed in the periphery of the NFL during embyrogenesis but becomes widespread throughout the NFL with increasing development (Au et al. 2002). Thus the sorting of axons within the NFL likely involves the axons interacting with different subpopulations of OECs which themselves have to migrate to the appropriate regions. Here we have observed for the first time that central OECs undergoing cell-cell contact result in a mix of responses in vitro: adhesion, repulsion or cross-over, indicating that central OECs respond differentially to each other.

We further examined subpopulations of central OECs from the different anatomical locations within the olfactory bulb and found that these OECs did indeed respond differentially to cell-cell contact. The rostral NFL consists of a prominent outer and inner NFL. The outer NFL is the region where axons defasciculate and sort out whereas the inner NFL is the region where axons refasciculate and project to glomeruli (Franceschini and Barnett 1996). The OECs in these layers have different antigenic profiles (Windus et al. 2007) and are thought to contribute differing roles to axon guidance. We analysed the OECs from the rostral NFL as a single culture of cells as it was not possible to dissect out the inner NFL from the outer NFL. However,

the differing roles of OECs in these two layers of the NFL were reflected in our in vitro assays with rostral OECs displaying a mix of adhesion, repulsion and cross-over. Moreover, irrespective of the age of the tissue from which they were derived, rostral OECs consistently displayed these three different types of behaviour. This suggests that the rostral region of the NFL may be important in continually sorting incoming coalescent axon bundles from the peripheral nerve. In contrast, the NFL from the dorsal and caudal regions of the NFL is much more compact without a clear distinction between inner and outer NFL. OECs derived from the caudal and dorsal NFL displayed a shift towards more adhesive responses that increased with the developmental age. Axons that project to these regions of the NFL have already undergone the majority of sorting in the rostral NFL. Thus, because there is less need for a complex sorting process in the dorsal and caudal NFL these OECs are likely to be more involved in the maintenance (adhesion) of established pathways and are likely to have a reduced role in sorting.

We have previously reported that peripheral OECs exhibit, highly dynamic lamellipodia along their shafts and are important cell mechanisms for initiating cell-cell interactions and mediating cell migration (Cao et al. 2006). We have now shown that these highly motile plasma membrane protrusions also exist on central OEC shafts and are intrinsic in regulating cell-cell interactions. In contrast to lamellipodial waves on peripheral OECs, which predominantly regulate adhesion (Windus et al. 2007), the lamellipodial waves on central OECs mediate a mix of adhesive, repulsive and cross-over behaviours.

Consistent with previous reports (Cao et al. 2006) and similar to peripheral OECs (Nodari et al. 2007) we have confirmed that GDNF stimulates wave activity and the migration of central OECs. This was confirmed when we found that GDNF increased the activity and size of lamellipodial waves. Moreover, this behaviour was mediated through the JNK and SRC kinases as recently reported for GDNF stimulation of OEC migration (Pankov et al. 2005). These results provide a clear link between wave activity and the migration rate of central OECs. We found however that GDNF does not alter intrinsic behaviours of central OECs associated with cell-cell contact.

While similar structures to that of lamellipodial waves have been reported on other cells types including Schwann cells (Nodari et al. 2007) and fibroblasts (Pankov et al. 2005), the role of lamellipodial waves on OECs are distinctly different. The role of radial lamellae on Schwann cells has been implicated with myelinating peripheral axons , whereas peripheral lamellae on fibroblasts are involved in regulating the direction of migration . We predicted instead that lamellipodial waves on central OECs are a unique mechanism by which molecular/receptor complexes are presented to surrounding cells and which lead to the rapid identification of neighbouring cells. This was confirmed when we inhibited lamellipodial wave formation via the Mek pathway, which causes collapse of the waves but maintains the activity of the leading edge. Without active lamellipodial waves, central OECs ceased to respond to each other during cell-cell contact (Fig. 7A). Thus the lamellipodial waves act independently of the leading edge and are essential for OEC cell recognition and mediating the response to cell-cell contact. Future work will determine the signalling molecules which are present on lamellipodial waves that are responsible for mediating OEC identification.

In summary, peripheral and central OECs display intrinsically different patterns of behaviour during cell-cell contact and these behaviours are mediated by lamellipodial waves. These behaviours differ depending on both the topographical location and the age of the tissue from which OECs are derived. Peripheral OECs are a homogeneous population, whereas central OECs are a heterogeneous population which display different behaviours that alter with developmental age. Importantly, the heterogeneity of responses by central OECs is mediated by lamellipodial waves. How these fundamental differences in intrinsic OEC properties affect axon regeneration is the work of future studies.

ACKNOWLEDGMENTS

This work was supported by grant from the National Health and Medical Research Council to J.S and B.K (Grant number 511006), by funding to the National Centre for Adult Stem Cell Research from the Australian Government Department of Health and Aging (A.M.S.) and an Australian Postgraduate Award to L.W.

REFERENCES

Astic L, Pellier-Monnin V, Godinot F. 1998. Spatio-temporal patterns of ensheathing cell differentiation in the rat olfactory system during development. Neuroscience 84(1):295-307.

Au E, Roskams AJ. 2003. Olfactory ensheathing cells of the lamina propria in vivo and in vitro. Glia 41(3):224-36.

Au WW, Treloar HB, Greer CA. 2002. Sublaminar organization of the mouse olfactory bulb nerve layer. J Comp Neurol 446(1):68-80.

Bailey MS, Puche AC, Shipley MT. 1999. Development of the olfactory bulb: evidence for glia-neuron interactions in glomerular formation. J Comp Neurol 415(4):423-48.

Barnett SC, Hutchins AM, Noble M. 1993. Purification of olfactory nerve ensheathing cells from the olfactory bulb. Dev Biol 155(2):337-50.

Bennett BL, Sasaki DT, Murray BW, O'Leary EC, Sakata ST, Xu W, Leisten JC, Motiwala A, Pierce S, Satoh Y and others. 2001. SP600125, an anthrapyrazolone inhibitor of Jun N-terminal kinase. Proc Natl Acad Sci U S A 98(24):13681-6.

Cao L, Su Z, Zhou Q, Lv B, Liu X, Jiao L, Li Z, Zhu Y, Huang Z, Huang A and others. 2006. Glial cell line-derived neurotrophic factor promotes olfactory ensheathing cells migration. Glia 54(6):536-44.

Chuah MI, Au C. 1991. Olfactory Schwann cells are derived from precursor cells in the olfactory epithelium. J Neurosci Res 29(2):172-80.

Danciger E, Mettling C, Vidal M, Morris R, Margolis F. 1989. Olfactory marker protein gene: its structure and olfactory neuron-specific expression in transgenic mice. Proc Natl Acad Sci U S A 86(21):8565-9.

Doucette JR. 1984. The glial cells in the nerve fiber layer of the rat olfactory bulb. Anat Rec 210(2):385-91.

Doucette JR. 1989. Development of the nerve fiber layer in the olfactory bulb of mouse embryos. J Comp Neurol 285(4):514-27.

Doucette JR. 1990. Glial influences on axonal growth in the primary olfactory system. Glia 3(6):433-49.

Farbman AI, Squinto LM. 1985. Early development of olfactory receptor cell axons. Brain Res 351(2):205-13.

Franceschini I, Barnett S. 1996. Low-affinity NGF-receptor and E-N-CAM expression define two types of olfactory nerve ensheathing cells that share a common lineage. Dev Biol 173(1):327-343.

Gong Q, Bailey MS, Pixley SK, Ennis M, Liu W, Shipley MT. 1994. Localization and regulation of low affinity nerve growth factor receptor expression in the rat olfactory system during development and regeneration. J Comp Neurol 344(3):336-48.

Hanke JH, Gardner JP, Dow RL, Changelian PS, Brissette WH, Weringer EJ, Pollok BA, Connelly PA. 1996. Discovery of a novel, potent, and Src family-selective tyrosine kinase inhibitor. Study of Lck- and FynT-dependent T cell activation. J Biol Chem 271(2):695-701.

Huang ZH, Wang Y, Cao L, Su ZD, Zhu YL, Chen YZ, Yuan XB, He C. 2008. Migratory properties of cultured olfactory ensheathing cells by single-cell migration assay. Cell Res 18(4):479-90.

Jani HR, Raisman G. 2004. Ensheathing cell cultures from the olfactory bulb and mucosa. Glia 47(2):130-7.

Kumar R, Hayat S, Felts P, Bunting S, Wigley C. 2005. Functional differences and interactions between phenotypic subpopulations of olfactory ensheathing cells in promoting CNS axonal regeneration. Glia 50(1):12-20.

Margolis FL. 1972. A brain protein unique to the olfactory bulb. Proc Natl Acad Sci U S A 69(5):1221-4.

Mombaerts P, Wang F, Dulac C, Chao SK, Nemes A, Mendelsohn M, Edmondson J, Axel R. 1996. Visualizing an olfactory sensory map. Cell 87(4):675-86.

Nodari A, Zambroni D, Quattrini A, Court FA, D'Urso A, Recchia A, Tybulewicz VL, Wrabetz L, Feltri ML. 2007. {beta}1 integrin activates Rac1 in Schwann cells to generate radial lamellae during axonal sorting and myelination. J Cell Biol 177(6):1063-75.

Pankov R, Endo Y, Even-Ram S, Araki M, Clark K, Cukierman E, Matsumoto K, Yamada KM. 2005. A Rac switch regulates random versus directionally persistent cell migration. J Cell Biol 170(5):793-802.

Schwarting GA, Kostek C, Ahmad N, Dibble C, Pays L, Puschel AW. 2000. Semaphorin 3A is required for guidance of olfactory axons in mice. J Neurosci 20(20):7691-7.

St John JA, Key B. 1999. Expression of galectin-1 in the olfactory nerve pathway of rat. Brain Res Dev Brain Res 117(2):171-8.

St John JA, Key B. 2001. EphB2 and two of its ligands have dynamic protein expression patterns in the developing olfactory system. Brain Res Dev Brain Res 126(1):43-56.

Storan MJ, Magnaldo T, Biol-N'Garagba MC, Zick Y, Key B. 2004. Expression and putative role of lactoseries carbohydrates present on NCAM in the rat primary olfactory pathway. J Comp Neurol 475(3):289-302.

Treloar HB, Feinstein P, Mombaerts P, Greer CA. 2002. Specificity of glomerular targeting by olfactory sensory axons. J Neurosci 22(7):2469-77.

Valverde F, Santacana M, Heredia M. 1992. Formation of an olfactory glomerulus: morphological aspects of development and organization. Neuroscience 49(2):255-75.

Vincent AJ, Taylor JM, Choi-Lundberg DL, West AK, Chuah MI. 2005a. Genetic expression profile of olfactory ensheathing cells is distinct from that of Schwann cells and astrocytes. Glia 51(2):132-47.

Vincent AJ, West AK, Chuah MI. 2005b. Morphological and functional plasticity of olfactory ensheathing cells. J Neurocytol 34(1-2):65-80.

Whitesides JG, 3rd, LaMantia AS. 1996. Differential adhesion and the initial assembly of the mammalian olfactory nerve. J Comp Neurol 373(2):240-54.

Windus LC, Claxton C, Allen CL, Key B, St John JA. 2007. Motile membrane protrusions regulate cell-cell adhesion and migration of olfactory ensheathing glia. Glia 55(16):1708-19.

FIGURE LEGENDS

Figure 1. OECs are a heterogeneous population. (A) A diagram depicting the olfactory system. In the PNS, OECs ensheathe primary olfactory axons in tightly fasciculated bundles. Once they reach the CNS, OECs contribute to the defasciculation, sorting and refasciculation of the olfactory axons. Panels B-E show coronal sections through the olfactory bulb and olfactory nerve with dorsal to the top and lateral to the right. (B) Low magnification of the olfactory bulb depicting OECs that reside in the nerve fibre layer (NFL) of the S100ß-DsRed adult mouse. (C) A higher magnification view of the NFL. DsRed-expressing OECs (red) are present throughout the NFL, whereas S100ß detected by antibody staining (green) is present in the outer NFL (oNFL). (D) The OECs of the inner NFL (iNFL) express NPY, whereas OECs in the oNFL do not. (E) Anti-p75 is clearly expressed by OECs present in the peripheral olfactory nerve (ON) and sparsely throughout the oNFL. (F) A section through the olfactory mucosa shows that peripheral OECs form tight circular fascicles (arrow) in the lamina propria (LP). Panels G-H show primary olfactory axons in vitro grown on monolayers of either central (G) or peripheral (I) derived OECs. When plated on central OECs, axons are spatially dispersed (H, arrows) while axons grown on peripheral OECs remain highly fasciculated (J, arrow). CNS, central nervous system; PNS peripheral nervous system; GL glomerular layer; OE Olfactory epithelium; ON olfactory nerve. Scale bar is 300 μm in B; 75 μm in C-F; 35 μm in G-J.

Figure 2. OEC cell-cell interactions in vitro result in a mix of responses. Centrally derived OECs display three specific behaviours during cell-cell interaction in vitro. (A) Adhesion: expression of S100ß-DsRed identifies two interacting OECs. The leading edge (arrow) is in contact with the shaft (asterisk) of a second OEC. Time-lapse differential inference contrast (DIC) images reveal that a lamellipodial wave was present at the point of contact (00.00, dotted line; 04.17, arrow) between the two processes. The leading edge interacted with the lamellipodial wave and then proceeded to align and adhere to the shaft of the second process (04.17, unfilled arrowhead). The shaft of the second OEC then retracted (09.27, arrow). The lamellipodial wave and leading edge actively interacted (16.57, arrowhead) resulting in adhesion between the two OECs (45.16, asterisk). Sequences are taken from Supplemental Movie 1. (B) Repulsion: a DIC image revealed an active leading edge of a central OEC (arrow) migrating towards the shaft of a second OEC process (asterisk). A lamellipodial wave emerged (demarcated by dotted line) and briefly interacted with the leading edge (16.42, arrow) before the leading edge retracted (33.42, arrow). Sequences are taken from Supplemental Movie 2. (C) Cross-over; whereby two OECs grow over each other without perturbation. A wave (arrowhead) present on a DsRed positive OEC made contact with the shaft of a second DsRed-positive OEC. Following contact with the second cell, the wave collapsed (06.40, arrowhead). Further along the shaft a second wave emerged (21.20, unfilled arrowhead), travelled in a retrograde direction and contacted the shaft of the second OEC which again resulted in collapse (35.19, arrow) of the lamellipodial wave. The OEC continued to grow over the second OEC without any adherent or repellent activity (40.00). Sequences are taken from Supplemental Movie 3. Time indicated is in min and sec. Scale bar = 20 μm. (D) Peripheral OECs derived from embryonic,

postnatal or adult tissue overwhelmingly displayed adhesive events; $p<0.001$ Chi Squared and ***$p<0.0015$ post-hoc Fisher's exact test. (E) Cell-cell contact of central OECs resulted in an even mix of adhesion, repulsion or cross-over events when derived from embryonic tissue, but changed significantly when derived from postnatal or adult tissue; $p<0.05$ Chi Squared and *$p<0.05$ post-hoc Fisher's exact test.

Figure 3. The olfactory bulb develops in a distinct rostral to caudal gradient. In OMP-ZsGreen x S100ß-DsRed mice, primary olfactory axons (green) and OECs (red) are clearly visible. (A) At E17 the olfactory bulb displays a distinct bulbar shape with a partial laminar organisation of the nerve fibre layer (NFL). The transition zone (arrowheads) between the PNS and CNS occurs in the ventral and rostral region of the olfactory bulb (OB). The NFL in the ventral portion of the OB is noticeably thicker and nascent glomeruli are detectable (B, arrowhead), while in the caudal region they are not yet detectable (C, arrowhead). (D) At P2 there is a distinct increase in NFL organisation with a distinguishable NFL and glomerular layer (GL). The ventral region (E arrowhead) has developed a band of glomeruli, while the caudal region is beginning to develop a thinly populated region of nascent glomeruli (F, arrowhead). (G) The ventral region of the olfactory bulb in adult (+ 5 weeks) mice is thickly populated with well formed glomeruli (H, arrowheads) while the caudal region remains thinly populated (I, arrowhead). Central OECs from different topographical areas have dissimilar responses to cell-cell contact in vitro. (J-M) Bar graphs depict the resultant behaviour of interacting central OECs derived from the (J) rostral, (K) dorsal, (L) ventral, and (M) caudal olfactory bulb tissue; $p<0.001$ Chi Squared and *$p<0.05$; ** $p<0.01$; *** $p<0.001$ post-hoc Fisher's exact test. GL, glomerular layer; NFL, nerve fibre layer. Scale bar = 100 µm in A,D,G, 30 µm in B,C,E,F,H,I.

Figure 4. Anterograde and retrograde travel of lamellipodial waves on isolated central derived OECs in vitro. Panels show a DsRed-expressing central OEC with lamellipodial waves. (A) A DIC image reveals that a single lamellipodial wave (dashed line) was present on the shaft of the process and was distinct from the leading edge (asterisk). The cell strongly expressed DsRed fluorescence and subsequent time-lapse imaging revealed that several lamellipodial waves formed along the shaft. A single lamellipodial wave formed on the shaft and moved in a retrograde direction (00.02.21 – 00.24.41,arrowhead). A second wave formed (00.46.22, dashed line) and moved in an anterograde direction (00.53.26, unfilled arrowhead) toward a third lamellipodial wave (00.53.26, dashed line) where they merged together (01.04.26, arrow) to form a single lamellipodial wave. Sequences are taken from Supplemental Movie 4. Time indicated is in hr, min and sec. Scale bar = 20 μm. Resultant cellular behaviour following initial cell-cell contact when a lamellipodial wave was present at the site of contact was quantified for (B) peripheral OECs and (C) central OECs; $p<0.001$ Chi Squared and $*p<0.05$, $***p<0.001$ post-hoc Fisher's exact test.

Figure 5. GDNF influences central OEC cell migration and wave activity. (A) Central OECs migrate at higher rates when challenged with 20 ng/ml of GDNF; the addition of JNK (9SP600125) or SRC (PP2) inhibitors decreased migration of OECs; (n=11-20); $p<0.05$ Kruskal-Wallis test and $*p<0.05$, post-hoc Dunn's Multiple Comparison test. (B) Percentage of cells with lamellipodial waves when challenged with GDNF and NGF; (n=11-20); $p<0.05$ Chi Squared and $*p<0.05$ post-hoc Fisher's exact test. (C) Quantification of the surface area of lamellipodial waves on isolated OECs

challenged with GDNF; (n=11-20); $p<0.01$ Kruskal-Wallis test and $*p<0.05$, $**p<0.01$ post-hoc Dunn's Multiple Comparison test. Error bars denote the standard error of mean. (D) Addition of GDNF dramatically increased the size of lamellipodial waves on OECs; scale bar = 10 µm. (E) Inhibition of JNK (by SP600125) or SRC (by PP2) alone reduced the occurrence of lamellipodial waves; whereas GDNF alone increased the occurrence of waves. When inhibitors were applied in combination with GDNF the phenotype was rescued. Incubation with the inactive analogue PP3 had no effect on wave frequency compared to controls; (n= 11-22) for all treatments; $p<0.01$ Chi Squared and $*p<0.05$ $**p<0.01$ post-hoc Fisher's exact test. (F) The addition of GDNF did not alter the mix of behaviours of interacting OECs (n=7-15; $p>0.05$).

Figure 6. Inhibition of wave activity via Mek alters central OEC behaviour. (A) Percentage of active lamellipodial waves and leading edge activity on isolated OECs when challenged with Rac 1 inhibitor (NSC23766); (n=15-20); $p<0.05$ Chi Squared and $*p<0.05$ post-hoc Fisher's exact test. (B) Addition of Rac 1 inhibited leading edge formation (arrow) while wave formation persisted (arrowhead); scale bar is 10 µm. (C) Quantification of the migration rates of central OECs with addition of Rac 1; (n=15-20); $p<0.05$ Kruskal-Wallis test and $*p<0.05$ post-hoc Dunn's Multiple Comparison test; error bars denote the standard error of mean. (D) Addition of Rac1 did not alter central OEC behaviour during cell-cell contact (n=7-15). (E) Percentage of active lamellipodial waves and leading edge activity on isolated OECs when challenged with Mek inhibitor (Ethanolate U0126); (n=15-20); $p<0.01$ Chi Squared, and $*p<0.05$, $**p<0.001$ post-hoc Fisher's exact test. (F) Addition of Mek inhibited wave formation while leading edge activity persisted (arrowhead); scale bar 10 µm. (G) Quantification of the migration rates of central OECs with addition of Mek;

(n=16-20); $p<0.05$ Kruskal-Wallis test and $*p<0.05$ post-hoc Dunn's Multiple Comparison test; error bars denote the standard error of mean. (H) With the addition of Mek, OECs no longer responded to each other; cross-over events became the predominant behaviour; (n=7-15); $p<0.05$ Chi Squared, and $*p<0.05$ post-hoc Fisher's exact test.

Figure 7. Lamellipodial waves regulate central OEC behaviour during cell-cell contact. (A) During cell-cell contact between peripheral OECs, the presence of lamellipodial waves and an active leading edge results in the predominant behaviour of cell-cell adhesion. (B) During cell-cell contact between central OECs, there is a mix of behaviours; adhesion, repulsion and cross-over (no response). (C) In the absence of the leading edge the behaviour of interacting OECs is regulated by lamellipodial waves and remains heterogeneous in nature. (D) In the absence of lamellipodial waves however, OECs do not respond to each other and the resultant behaviour following cell-cell interaction is predominantly cross-over.

SUPPLEMENTARY MOVIE LEGENDS

Movie 1: Central OECs adhere to one another during cell-cell contact. Contact between the leading edge of one OEC and the shaft of another OEC resulted in the formation of a lamellipodial wave. A subsequent retraction of the shaft of one OEC is observed allowing the two leading edges to merge and cell-cell adhesion takes place. Time is recorded in min, sec and msec. Selected frames shown in Fig. 2A.

Movie 2: Central OECs repel from each other during cell-cell contact. The leading edge of an OEC moved toward a second OEC which extended a lamellipodial wave

with filopodia that interacted with the leading edge. Despite a brief interaction, the leading edge retracted within minutes. Time is recorded in hr, min and sec. Selected cropped frames are shown in Fig. 2B.

Movie 3: Central OECs also display non-responsive behaviour during cell-cell contact. As OECs crossed over, the lamellipodial waves that emerged on the shaft of the cell collapsed following contact with the adjacent cell. A lamellipodial wave extended a single filopodium which contacted the shaft of the second OEC resulting in collapse of the wave. Both OECs continued to exist without obvious adhesion or repulsion occurring. Time is recorded min, sec and msec. Selected cropped frames are shown in Fig. 2C.

Movie 4: Motile lamellipodial waves travel in both an anterograde and/or retrograde direction along a central OEC. Several lamellipodial waves appear along the shaft of an isolated OEC process. The initial wave travelled in a retrograde direction while the second wave developed and travelled anterograde prior to merging with a third lamellipodial wave. Merged wave subsequently moved retrograde toward the cell body. Time is recorded in hr, min and sec. Selected cropped frames are shown in Fig. 4A.

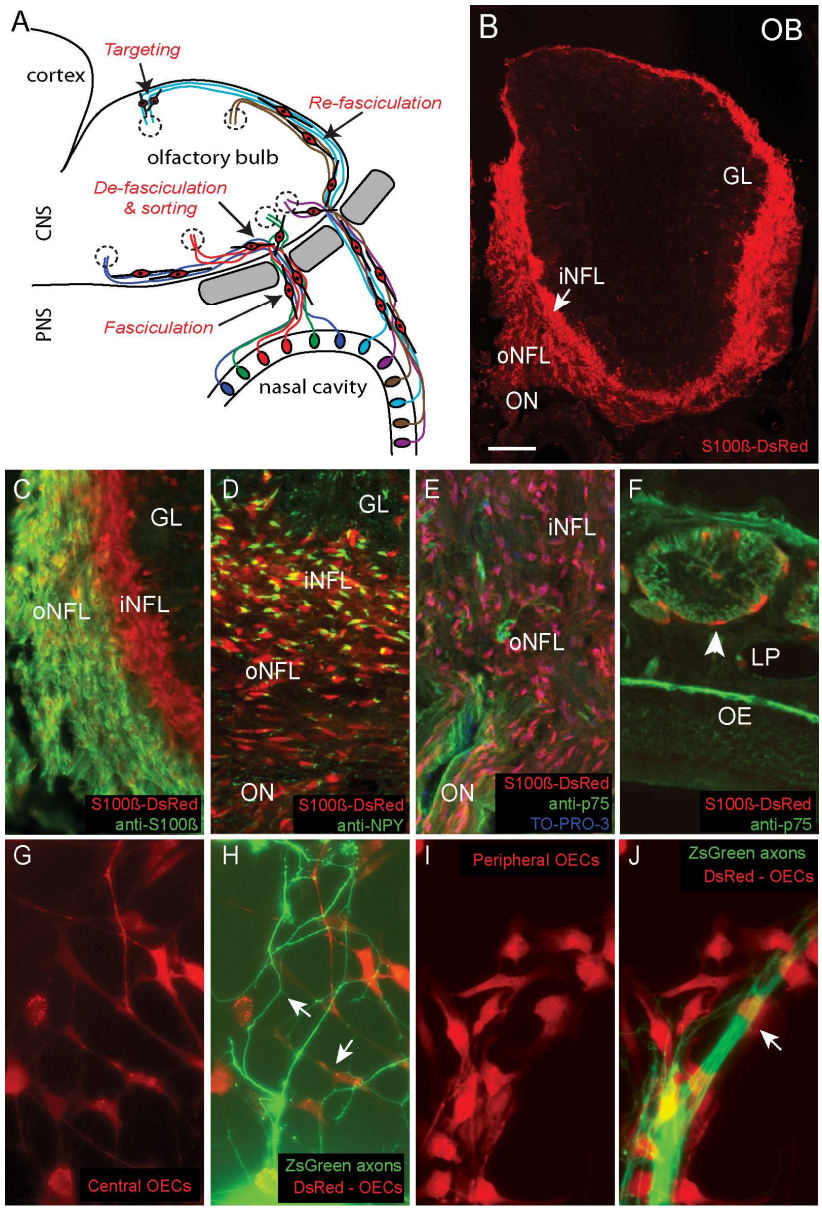

Figure 1. OECs are a heterogeneous population. (A) A diagram depicting the olfactory system. In the PNS, OECs ensheathe primary olfactory axons in tightly fasciculated bundles. Once they reach the CNS, OECs contribute to the defasciculation, sorting and refasciculation of the olfactory axons. Panels B-E show coronal sections through the olfactory bulb and olfactory nerve with dorsal to the top and lateral to the right. (B) Low magnification of the olfactory bulb depicting OECs that reside in the nerve fibre layer (NFL) of the S100ß-DsRed adult mouse. (C) A higher magnification view of the NFL. DsRed-expressing OECs (red) are present throughout the NFL, whereas S100ß detected by antibody staining (green) is present in the outer NFL (oNFL). (D) The OECs of the inner NFL (iNFL) express NPY, whereas OECs in the oNFL do not. (E) Anti-p75 is clearly expressed by OECs present in the peripheral olfactory nerve (ON) and sparsely throughout the oNFL. (F) A section through the olfactory mucosa shows that peripheral OECs form tight circular fascicles (arrow) in the lamina propria (LP). Panels G-H show primary olfactory axons in vitro grown on monolayers of either central (G) or peripheral (I) derived OECs. When plated on central OECs, axons are spatially

dispersed (H, arrows) while axons grown on peripheral OECs remain highly fasciculated (J, arrow). CNS, central nervous system; PNS peripheral nervous system; GL glomerular layer; OE Olfactory epithelium; ON olfactory nerve. Scale bar is 300 μm in B; 75 μm in C-F; 35 μm in G-J.
136x200mm (300 x 300 DPI)

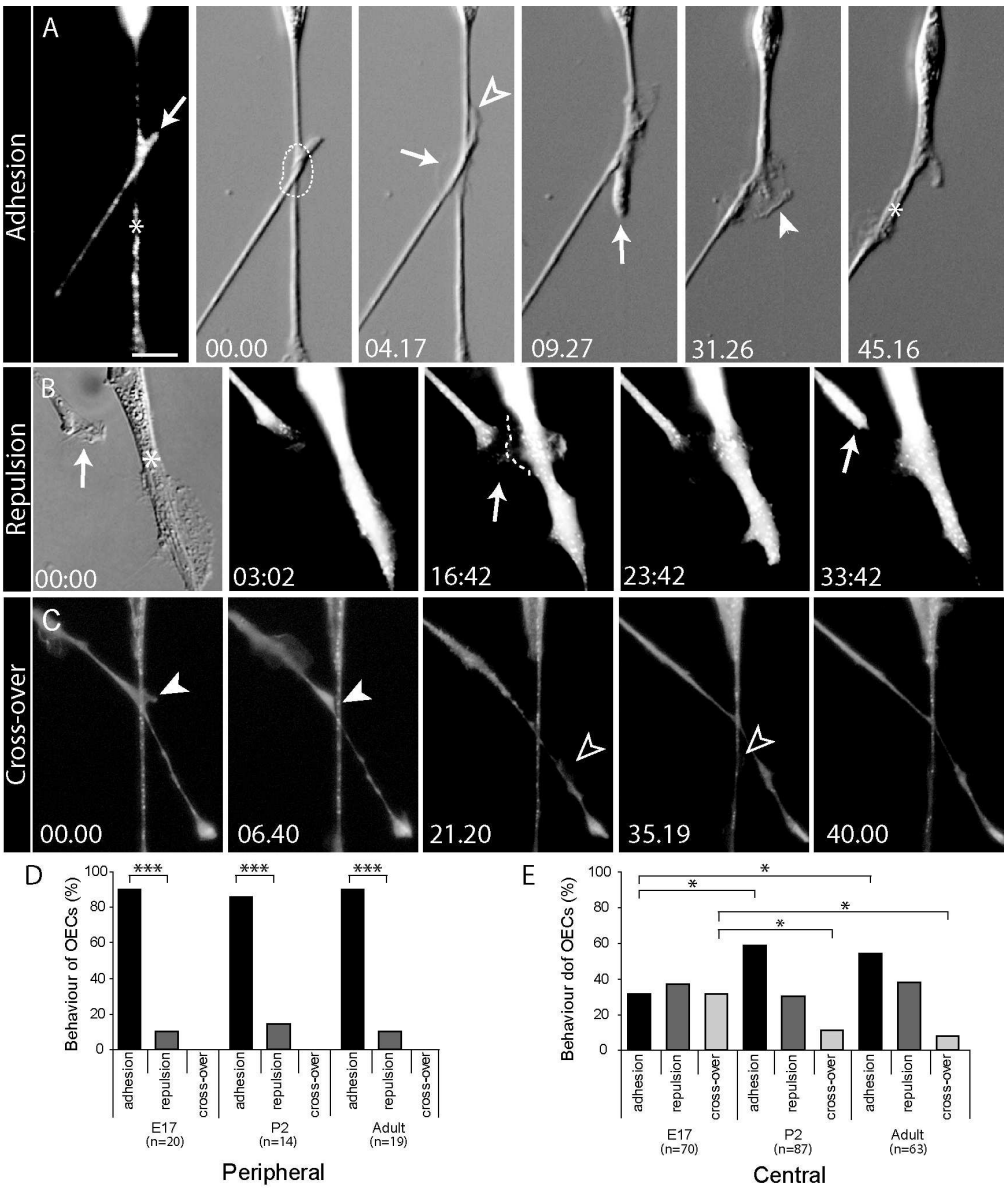

Figure 2. OEC cell-cell interactions in vitro result in a mix of responses. Centrally derived OECs display three specific behaviours during cell-cell interaction in vitro. (A) Adhesion: expression of S100ß-DsRed identifies two interacting OECs. The leading edge (arrow) is in contact with the shaft (asterisk) of a second OEC. Time-lapse differential inference contrast (DIC) images reveal that a lamellipodial wave was present at the point of contact (00.00, dotted line; 04.17, arrow) between the two processes. The leading edge interacted with the lamellipodial wave and then proceeded to align and adhere to the shaft of the second process (04.17, unfilled arrowhead). The shaft of the second OEC then retracted (09.27, arrow). The lamellipodial wave and leading edge actively interacted (16.57, arrowhead) resulting in adhesion between the two OECs (45.16, asterisk). Sequences are taken from Supplemental Movie 1. (B) Repulsion: a DIC image revealed an active leading edge of a central OEC (arrow) migrating towards the shaft of a second OEC process (asterisk). A lamellipodial wave emerged (demarcated by dotted line) and briefly interacted with the leading edge (16.42, arrow) before the leading edge retracted (33.42, arrow). Sequences are taken

from Supplemental Movie 2. (C) Cross-over; whereby two OECs grow over each other without perturbation. A wave (arrowhead) present on a DsRed positive OEC made contact with the shaft of a second DsRed-positive OEC. Following contact with the second cell, the wave collapsed (06.40, arrowhead). Further along the shaft a second wave emerged (21.20, unfilled arrowhead), travelled in a retrograde direction and contacted the shaft of the second OEC which again resulted in collapse (35.19, arrow) of the lamellipodial wave. The OEC continued to grow over the second OEC without any adherent or repellent activity (40.00). Sequences are taken from Supplemental Movie 3. Time indicated is in min and sec. Scale bar = 20 μm. (D) Peripheral OECs derived from embryonic, postnatal or adult tissue overwhelmingly displayed adhesive events; $p<0.001$ Chi Squared and ***$p<0.0015$ post-hoc Fisher's exact test. (E) Cell-cell contact of central OECs resulted in an even mix of adhesion, repulsion or cross-over events when derived from embryonic tissue, but changed significantly when derived from postnatal or adult tissue; $p<0.05$ Chi Squared and *$p<0.05$ post-hoc Fisher's exact test.
146x173mm (300 x 300 DPI)

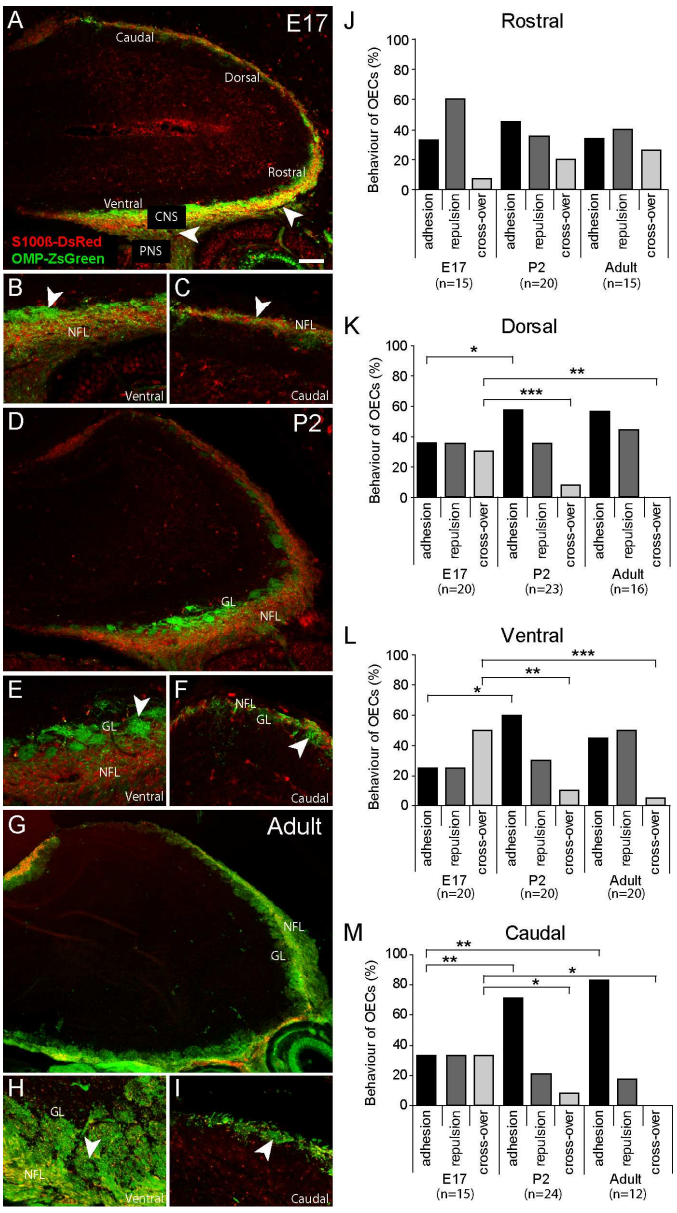

Figure 3. The olfactory bulb develops in a distinct rostral to caudal gradient. In OMP-ZsGreen x S100ß-DsRed mice, primary olfactory axons (green) and OECs (red) are clearly visible. (A) At E17 the olfactory bulb displays a distinct bulbar shape with a partial laminar organisation of the nerve fibre layer (NFL). The transition zone (arrowheads) between the PNS and CNS occurs in the ventral and rostral region of the olfactory bulb (OB). The NFL in the ventral portion of the OB is noticeably thicker and nascent glomeruli are detectable (B, arrowhead), while in the caudal region they are not yet detectable (C, arrowhead). (D) At P2 there is a distinct increase in NFL organisation with a distinguishable NFL and glomerular layer (GL). The ventral region (E arrowhead) has developed a band of glomeruli, while the caudal region is beginning to develop a thinly populated region of nascent glomeruli (F, arrowhead). (G) The ventral region of the olfactory bulb in adult (+ 5 weeks) mice is thickly populated with well formed glomeruli (H, arrowheads) while the caudal region remains thinly populated (I, arrowhead). Central OECs from different topographical areas have

dissimilar responses to cell-cell contact in vitro. (J-M) Bar graphs depict the resultant behaviour of interacting central OECs derived from the (J) rostral, (K) dorsal, (L) ventral, and (M) caudal olfactory bulb tissue; $p<0.001$ Chi Squared and *$p<0.05$; ** $p<0.01$; *** $p<0.001$ post-hoc Fisher's exact test. GL, glomerular layer; NFL, nerve fibre layer. Scale bar = 100 μm in A,D,G, 30 μm in B,C,E,F,H,I.
117x210mm (300 x 300 DPI)

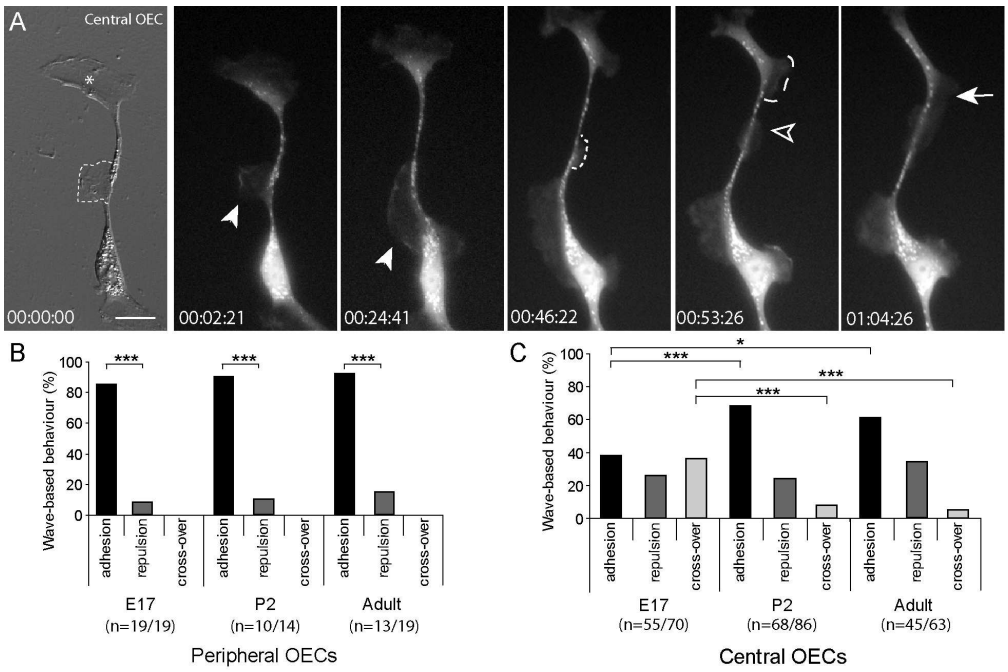

Figure 4. Anterograde and retrograde travel of lamellipodial waves on isolated central derived OECs in vitro. Panels show a DsRed-expressing central OEC with lamellipodial waves. (A) A DIC image reveals that a single lamellipodial wave (dashed line) was present on the shaft of the process and was distinct from the leading edge (asterisk). The cell strongly expressed DsRed fluorescence and subsequent time-lapse imaging revealed that several lamellipodial waves formed along the shaft. A single lamellipodial wave formed on the shaft and moved in a retrograde direction (00.02.21 – 00.24.41,arrowhead). A second wave formed (00.46.22, dashed line) and moved in an anterograde direction (00.53.26, unfilled arrowhead) toward a third lamellipodial wave (00.53.26, dashed line) where they merged together (01.04.26, arrow) to form a single lamellipodial wave. Sequences are taken from Supplemental Movie 4. Time indicated is in hr, min and sec. Scale bar = 20 μm. Resultant cellular behaviour following initial cell-cell contact when a lamellipodial wave was present at the site of contact was quantified for (B) peripheral OECs and (C) central OECs; $p<0.001$ Chi Squared and *$p<0.05$, ***$p<0.001$ post-hoc Fisher's exact test.
165x109mm (300 x 300 DPI)

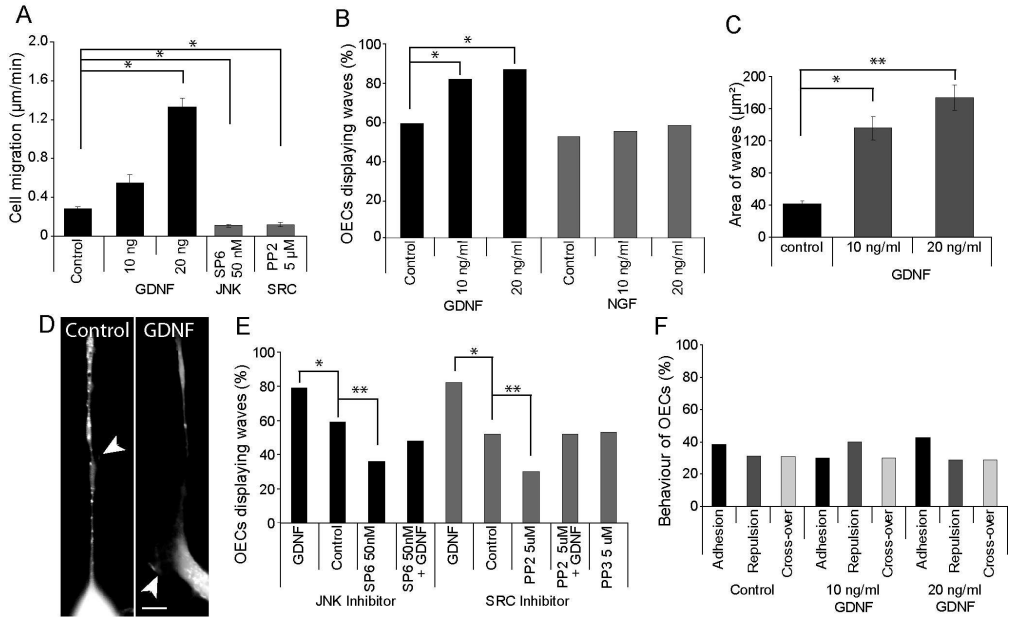

Figure 5. GDNF influences central OEC cell migration and wave activity. (A) Central OECs migrate at higher rates when challenged with 20 ng/ml of GDNF; the addition of JNK (9SP600125) or SRC (PP2) inhibitors decreased migration of OECs; (n=11-20); $p<0.05$ Kruskal-Wallis test and $*p<0.05$, post-hoc Dunn's Multiple Comparison test. (B) Percentage of cells with lamellipodial waves when challenged with GDNF and NGF; (n=11-20); $p<0.05$ Chi Squared and $*p<0.05$ post-hoc Fisher's exact test. (C) Quantification of the surface area of lamellipodial waves on isolated OECs challenged with GDNF; (n=11-20); $p<0.01$ Kruskal-Wallis test and $*p<0.05$, $**p<0.01$ post-hoc Dunn's Multiple Comparison test. Error bars denote the standard error of mean. (D) Addition of GDNF dramatically increased the size of lamellipodial waves on OECs; scale bar = 10 µm. (E) Inhibition of JNK (by SP600125) or SRC (by PP2) alone reduced the occurrence of lamellipodial waves; whereas GDNF alone increased the occurrence of waves. When inhibitors were applied in combination with GDNF the phenotype was rescued. Incubation with the inactive analogue PP3 had no effect on wave frequency compared to controls; (n= 11-22) for all treatments; $p<0.01$ Chi Squared and $*p<0.05$ $**p<0.01$ post-hoc Fisher's exact test. (F) The addition of GDNF did not alter the mix of behaviours of interacting OECs (n=7-15; $p>0.05$).
173x106mm (300 x 300 DPI)

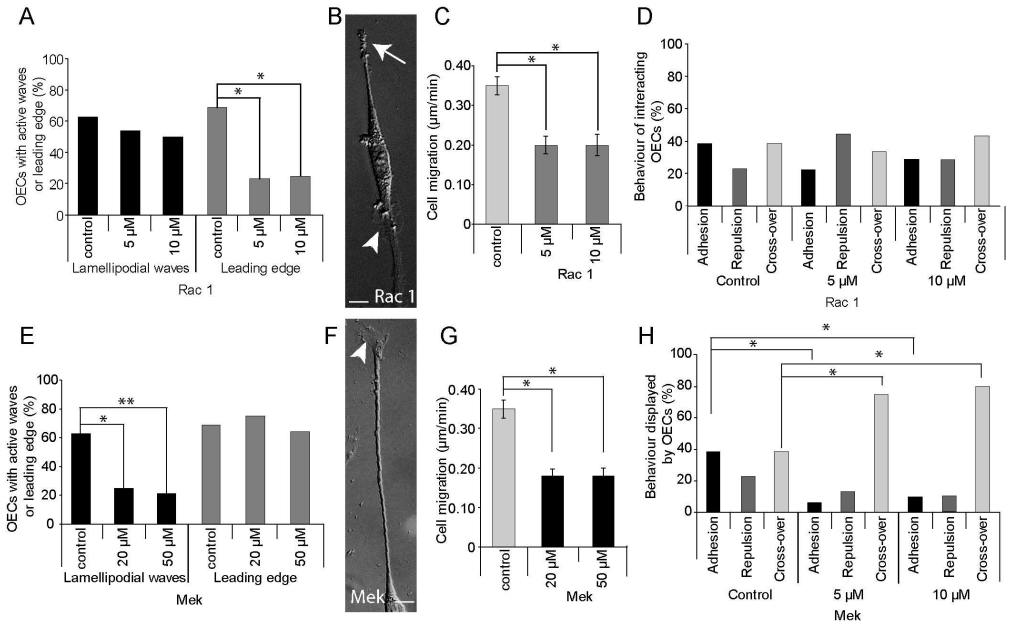

Figure 6. Inhibition of wave activity via Mek alters central OEC behaviour. (A) Percentage of active lamellipodial waves and leading edge activity on isolated OECs when challenged with Rac 1 inhibitor (NSC23766); (n=15-20); $p<0.05$ Chi Squared and *$p<0.05$ post-hoc Fisher's exact test. (B) Addition of Rac 1 inhibited leading edge formation (arrow) while wave formation persisted (arrowhead); scale bar is 10 µm. (C) Quantification of the migration rates of central OECs with addition of Rac 1; (n=15-20); $p<0.05$ Kruskal-Wallis test and *$p<0.05$ post-hoc Dunn's Multiple Comparison test; error bars denote the standard error of mean. (D) Addition of Rac1 did not alter central OEC behaviour during cell-cell contact (n=7-15). (E) Percentage of active lamellipodial waves and leading edge activity on isolated OECs when challenged with Mek inhibitor (Ethanolate U0126); (n=15-20); $p<0.01$ Chi Squared, and *$p<0.05$, **$p<0.001$ post-hoc Fisher's exact test. (F) Addition of Mek inhibited wave formation while leading edge activity persisted (arrowhead); scale bar 10 µm. (G) Quantification of the migration rates of central OECs with addition of Mek; (n=16-20); $p<0.05$ Kruskal-Wallis test and *$p<0.05$ post-hoc Dunn's Multiple Comparison test; error bars denote the standard error of mean. (H) With the addition of Mek, OECs no longer responded to each other; cross-over events became the predominant behaviour; (n=7-15); $p<0.05$ Chi Squared, and *$p<0.05$ post-hoc Fisher's exact test.
177x110mm (300 x 300 DPI)

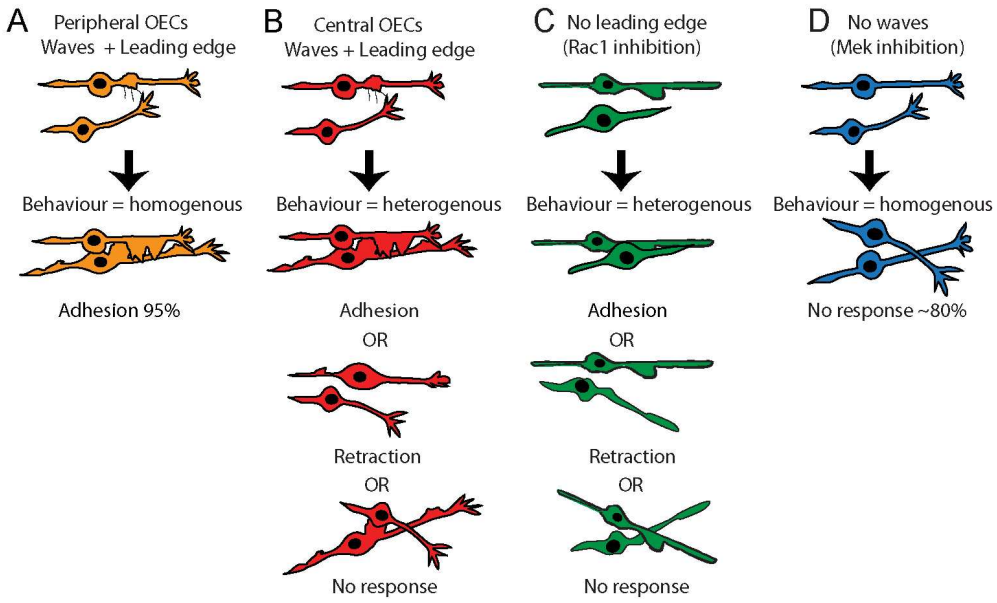

Figure 7. Lamellipodial waves regulate central OEC behaviour during cell-cell contact. (A) During cell-cell contact between peripheral OECs, the presence of lamellipodial waves and an active leading edge results in the predominant behaviour of cell-cell adhesion. (B) During cell-cell contact between central OECs, there is a mix of behaviours; adhesion, repulsion and cross-over (no response). (C) In the absence of the leading edge the behaviour of interacting OECs is regulated by lamellipodial waves and remains heterogeneous in nature. (D) In the absence of lamellipodial waves however, OECs do not respond to each other and the resultant behaviour following cell-cell interaction is predominantly cross-over.
130x77mm (300 x 300 DPI)